STUDIA UBB CHEMIA, LXXI, 2, 2026 (p. 147-170)
(RECOMMENDED CITATION)
DOI:10.24193/subbchem.2026.2.08

ADSORPTION OF METHYLENE BLUE ONTO RAW SECONDARY SEWAGE SLUDGE: ISOTHERM, KINETIC, AND CHARACTERIZATION STUDIES

Ilhaam KHATRI[a], Ashish TAMBI[b,*], Deepak Singh RAJAWAT[c]

ABSTRACT. The increased discharge of synthetic dyes into aquatic ecosystems has caused significant environmental concerns, prompting the search for sustainable adsorbents. Sewage sludge, an abundant by-product of wastewater treatment facilities, offers the opportunity for dye removal within a circular economy paradigm. This study investigates the potential of raw dried secondary treated sewage sludge as an effective adsorbent for the removal of methylene blue, a cationic dye, from aqueous solutions. The adsorbent was characterized by Fourier transform infrared spectroscopy, field emission scanning electron microscopy, and Brunauer–Emmett–Teller surface analysis to evaluate its morphology, functional groups and textural properties. Batch adsorption experiments examined the effects of pH, initial dye concentration, adsorbent dosage, particle size, and contact time on the removal efficiency. Optimal conditions were observed at pH 9, with 0.5 g of sewage sludge (particle size 0.5 mm) in 50 mL of 10 mg/L dye solution and a contact time of 30 minutes. The adsorption equilibrium data conformed best to the Langmuir isotherm model, with a maximum monolayer adsorption capacity of 14.08 mg/g. Kinetic studies indicated that the adsorption process followed the pseudo-second-order model (R^2=0.999), suggesting chemisorption as the predominant mechanism. The adsorbent also exhibited a pH-stabilizing behaviour, wherein the solution pH after adsorption shifted toward neutrality regardless of the initial pH, highlighting its suitability for practical wastewater treatment applications. The study demonstrates the potential of raw secondary treated sewage sludge as an eco-friendly adsorbent, aligning with sustainable wastewater treatment strategies.

Keywords: *Adsorption, dye removal, methylene blue, sewage sludge, wastewater treatment*

[a] *Department of Environmental Science, IIS (Deemed to be University), Jaipur, Rajasthan, India*
[b] *Amity School of Earth and Environmental Sciences, Amity University Punjab, Mohali, Punjab, India*
[c] *Department of Chemistry, IIS (Deemed to be University), Jaipur, Rajasthan, India*
* *Corresponding author: ashishtambi006@gmail.com*

1. INTRODUCTION

The textile industry makes a huge contribution to the global economy, but it is also a major source of environmental pollution due to the discharge of dye-laden wastewater. Textile processing makes considerable use of synthetic dyes to produce bright and diversified colours in fabrics. These dyes are usually highly stable and resistant to degradation, allowing them to persist in aquatic environments. Furthermore, textile businesses rely on considerable amounts of water, resulting in significant amounts of wastewater. For dyeing about a kg of fabric, 70-150 litres of freshwater are required [1].

During manufacturing operations, synthetic dyes like methylene blue (MB), a common cationic dye, are frequently released into water bodies because they are not completely bonded to textile fibres [2]. Studies show that around 50% of dyes used end up being released into the water bodies [3]. These colours disturb food chains, increase biochemical oxygen demand (BOD), and reduce dissolved oxygen (DO) in aquatic environments by restricting sunlight penetration, which hinders photosynthesis. Furthermore, their toxicity, carcinogenicity, and mutagenicity characteristics provide serious health risks [2].

Methylene blue (MB), in particular, is an aromatic heterocyclic compound known for its environmental persistence and potential toxicity. At high concentrations, it can cause adverse health effects in humans such as chest pain, headaches, abdominal discomfort, and methemoglobinemia [3]. Therefore, the removal of methylene blue from wastewater has garnered considerable attention. Various physicochemical techniques have been developed for dye removal, including coagulation, filtration, oxidation, and membrane separation. However, adsorption has emerged as one of the most effective and economical techniques due to its increased efficiency, simplicity, and broad applicability [4]. Activated carbon is a conventional adsorbent known for its excellent performance, but its high production and regeneration costs have driven the search for low-cost alternatives [5]. Global production of Sewage Sludge (SS), a by-product of municipal wastewater treatment, is enormous. 3.96 million tons of dry sludge are produced annually in India alone from the roughly 62,000 million litres of sewage per day (MLD) that are created, of which only around 20,120 MLD are treated [6]. The most popular methods for managing and disposing of sewage sludge are landfilling, land application, and incineration. All of these methods have serious disadvantages, including land degradation, soil contamination, and air pollution [7].

Despite the abundance of sewage sludge, its capacity as a low-cost adsorbent for colour removal has garnered limited attention. While prior research has investigated the conversion of sludge into biochar for dye

adsorption, such procedures typically require considerable energy inputs and operating expenditures, which may reduce the overall sustainability and economic viability of the process, especially for large-scale applications [8]. The potential of using raw sludge directly as a low-cost, readily available material has not been adequately assessed. Therefore, the current work is focused on the use of raw, dried sewage sludge with no chemical or thermal modification as an effective and affordable adsorbent for methylene blue removal from aqueous solutions. The main objectives of this research were to characterise and assess the adsorption capacity of raw sewage sludge for MB removal under various experimental factors. Adsorption isotherms and kinetic models were applied to assess the adsorption mechanism.

Unlike most studies that rely on thermally or chemically modified sludge, this work eliminates the need for energy-intensive or chemical pre-treatment, thereby significantly reducing operational costs and environmental impact. By directly repurposing sludge, the study aligns with circular economy principles, promoting a waste-to-resource approach that addresses both waste management and water pollution challenges.

2. MATERIALS AND METHODS

2.1. Dye Solution Preparation

Analytical grade methylene blue (MB) dye ($C_{16}H_{18}ClN_3S$) was obtained from Molychem India LLP, Mumbai (India). A stock solution of 500 mg/L was prepared using deionised water and diluted to obtain six initial working concentrations, i.e., 10, 20, 40, 50, 75 and 100 mg/L. The pH of the system was adjusted using 0.1 M NaOH (Merck Life Science Private Limited, Mumbai) and HCl (Thermo Fisher Scientific India Pvt. Ltd., Mumbai). All the reagents used were of analytical grade.

2.2. Collection and Preparation of Adsorbent

Dewatered secondary treated sewage sludge (SS) was collected from a nearby municipal wastewater treatment plant based on the Sequential Batch Reactor process located at Devri, Mansarovar, Jaipur, Rajasthan, India. The sludge was dried for 2-3 days, followed by oven drying at 105°C for 24 hours to ensure complete removal of moisture. The dried sludge was then crushed using a mortar and pestle and sieved to obtain a uniform particle size. The prepared sludge powder was stored in an airtight container for further use in batch adsorption studies.

2.3. Characterisation of Adsorbent

2.3.1. Fourier Transform Infrared Spectroscopy (FTIR)

FTIR analysis was performed using the Bruker FTIR Alpha 2 spectrometer to identify the functional groups present on the surface of the adsorbent before and after adsorption. The samples were analysed in the range of 4000–400 cm^{-1} with 4 cm^{-1} resolution using the KBr pellet method. Changes in peak intensities and positions were used to determine the interaction of functional groups with methylene blue dye molecules.

2.3.2. Scanning Electron Microscopy

The surface morphology and elemental composition of the dried sewage sludge were analysed using field emission scanning electron microscopy (FESEM). FESEM provided insights into the surface texture, porosity, and structural features of the sludge that might be helpful in adsorption.

2.3.3. Brunauer–Emmett–Teller (BET) Surface Area Analysis

Using nitrogen adsorption-desorption isotherms via BET analysis, the adsorbent's (before and after adsorption) specific surface area, pore volume, and pore size distribution were determined. To perform the measurements, a Quantachrome NOVA TouchWin v1.24 analyser was used. The SS sample for both before and after adsorption was degassed for approximately two hours at 150°C. The specific surface area was estimated using the produced isotherms, and the total pore volume was computed using the BET technique.

2.3.4. Determination of Point of Zero Charge (pH_{pzc})

The point of zero charge (pH_{pzc}) of the sewage sludge was determined by the pH drift method [9]. A series of 50 mL of 0.01 M NaCl solutions was adjusted to initial pH values ranging from 2 to 12 using 0.1 M HCl or NaOH. To each solution, 0.2 g of the dried adsorbent was added. The suspensions were then shaken at room temperature for 24 hours. The final pH values were recorded, and the difference between final and initial pH (ΔpH) was plotted against the initial pH. The point at which ΔpH = 0 was identified as the pH_{pzc} of the adsorbent.

2.4. UV–Vis Spectrophotometric Analysis of Methylene Blue

The concentration of methylene blue in aqueous solution was determined using a UV–Vis spectrophotometer (Shimadzu UV 1900i) by measuring the absorbance at the maximum wavelength (λmax) of 664 nm. A calibration curve was constructed using standard methylene blue solutions with concentrations

ranging from 0.5–10 mg/L. The absorbance values measured at 664 nm were plotted against the corresponding concentrations to obtain the calibration curve, which was subsequently used to determine the residual dye concentration in all adsorption experiments. The UV–Vis spectra of the standard solutions used for calibration are presented in Figure 1.

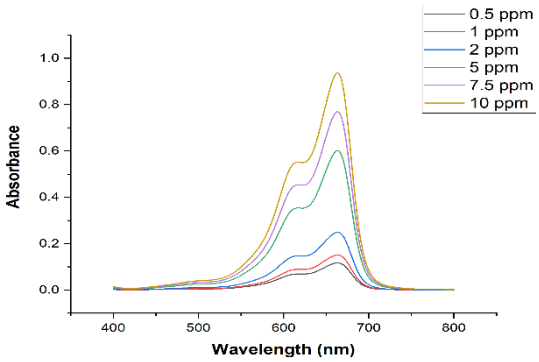

Figure 1. UV–Vis spectra of methylene blue standard solutions

3. BATCH ADSORPTION STUDY

Batch experiments were performed by adding 0.5 g of sewage sludge (SS) to 50 mL of methylene blue (MB) solution in 250 mL Erlenmeyer flasks. The flasks were agitated at 180 rpm in a rotary flask shaker (Icon Instruments Company, New Delhi) for 30 minutes and subsequently centrifuged at 3000 rpm for 10 minutes. For each adsorption experiment, the supernatant solution was analyzed using UV–Vis spectroscopy in the range of 400–800 nm, and the absorbance at 664 nm was used to determine the residual dye concentration. The effects of pH, initial dye concentration, particle size, adsorbent dosage, and contact time were analysed in the range of 3-11, 10-100 mg/L, 0.25-1 mm, 0.25-1 g, and 5-120 mins, respectively. The adsorption efficiency of sewage sludge and the amount of MB dye adsorbed were computed using equations (1) and (2) as mentioned below:

$$\% \text{ dye removal} = \left(\frac{C_o - C_f}{C_o}\right) * 100 \quad (1)$$

$$q_e = \left(\frac{C_o - C_f}{m}\right) * V \quad (2)$$

where C_o and C_f are the initial and final dye concentration (mg/L), q_e is the MB dye equilibrium concentration (mg/g), V is the volume of the dye solution, and m is the mass of adsorbent (g).

3.1. Adsorption Isotherm Models

The adsorption isotherms help in evaluating the correlation between q_e, i.e., the amount of adsorbed dye on the adsorbent (mg/g) and C_e, i.e., the concentration of dye adsorbed in the equilibrium phase (mg/L) in the liquid phase [10].

In the present study, adsorption mechanisms and the parameters involved in dye adsorption were investigated using two-parameter isotherms, including the Freundlich, Langmuir, Harkin-Jura, and Temkin isotherm models, to determine a specific relationship between dye in the liquid and solid phases—these models' experimental results over a broad range of concentrations and temperatures. The equations and their respective description to obtain the graphs are shown in Table 1.

Table 1. Adsorption isotherm models applied to the experimental data

Isotherm Model	Equation	Description	Parameters
Langmuir [10, 11]	$\frac{1}{q_e} = \frac{1}{K_L}.q_{max}.C_e + \frac{1}{q_{max}}$	q_e- amount of dye adsorbed at equilibrium q_{max}- maximum adsorption capacity K_L-adsorption energy C_e- concentration at equilibrium R_L- separation factor	K_L=intercept/slope q_{max}=1/intercept $R_L = 1/(1+K_LC_o)$
Freundlich [11]	$logq_e = logK_F + \frac{1}{n}logC_e$	q_e- adsorbent capacity at equilibrium C_e- concentration at equilibrium K_F- Freundlich constant *1/n*- relative adsorption capacity of the adsorbent	*1/n*= slope
Temkin [12, 13]	$q_e = B_T lnA_T + B_T lnC_e$	*T*- absolute temperature *R*- universal gas constant (8.314 J/mol·K) A_T- equilibrium binding constant b_T- heat of adsorption constant	$B_T = RT/b_T$
Harkin-Jura [11]	$\frac{1}{{q_e}^2} = \frac{B}{A} - \frac{1}{A}logC_e$	*B* and *A*- Harkin-Jura constants	

The Langmuir adsorption isotherm assumes that adsorption occurs on a homogeneous surface of the adsorbent and that the sites possess equal energy for adsorption. Further, it was assumed that adsorption proceeds until a monolayer is completed [5,10]. In contrast to the Langmuir isotherm, the Freundlich isotherm explains adsorption on heterogeneous surfaces and has different affinities. The Temkin isotherm determines whether the adsorption process is chemisorption or physisorption [13]. The model assumes the heat of adsorption decreases evenly as more pollutants are added to the surface [12]. The Harkin-Jura model is suitable for rough adsorbent surfaces where adsorption forms heterogeneous multi-layers and has different pore distributions [11].

3.2. Adsorption Kinetics

Experiments regarding adsorption kinetics were performed to determine the rate of adsorption. To investigate the kinetics of MB dye adsorption onto sewage sludge, Pseudo First-Order (PFO), Pseudo Second-Order (PSO), Elovich, and Intraparticle Diffusion (IPD) models were utilised, as shown in Table 2.

The Lagergren model (1898), also known as the Pseudo-first order (PFO) model, assumes that the mechanism involved in adsorption is physisorption, which is controlled by diffusion and mass transfer, while the Pseudo-second order (PSO) model assumes that the mechanism involved for adsorption is chemisorption (chemical sorption), which is a rate-limiting step [14]. The Elovich model is applied where the adsorbent's surface is heterogeneous, implying that adsorption occurs through chemisorption. The Weber-Morris model (1963) or Intra-particle diffusion (IPD**)** was applied to investigate the diffusion mechanism. This model helps in finding whether diffusion is the rate-limiting step for adsorption. The mathematical expressions for all the above-described models are provided in Table 2.

Table 2. Adsorption kinetic models applied to the experimental data [15]

Kinetic Model	Equation	Description
PFO	$ln\ (q_e - q_t) = ln\ q_e - k_1 t$	q_e- amount of dye adsorbed at equilibrium q_t- amount of dye adsorbed at time 't' k_1, k_2 and k_{id}- rate constants t- time α- initial adsorption coefficient β- desorption coefficient C_i- Intercept (boundary layer effect)
PSO	$t/q_t = (1/k_2 q_e^2) + t/q_e$	
Elovich	$q_t = \frac{1}{\beta} ln\ (\alpha\beta) + \frac{1}{\beta} ln\ t$	
IPD	$q_t = k_{id}\ .t^{1/2} + C_i$	

3.3. Thermodynamics study

To determine the thermodynamic parameters controlling the adsorption process, studies were carried out at 298, 308, and 318 K. As equilibrium was achieved, the dye solutions were centrifuged, and absorbance was taken at 664 nm using a UV-visible spectrophotometer. The thermodynamic parameters included are the change in Gibbs free energy (∆*G*), change in enthalpy (∆*H*), and change in entropy (∆*S*), which were calculated by the Clausius-Clapeyron equation (3) and the Gibbs free energy equation (4)

$$\ln K_d = \frac{\Delta S}{R} - \frac{\Delta H}{RT} \quad (3)$$

$$\Delta G = \Delta H - T\Delta S \quad (4)$$

where K_d represents the constant associated with the Langmuir isotherm, R denotes the universal gas constant valued at 8.314 $J \cdot mol^{-1} K^{-1}$, and T indicates temperature (K). The expression used to determine the distribution coefficient (K_d) is given by equation (5).

$$K_d = q_e/C_e \quad (5)$$

4. RESULTS AND DISCUSSIONS

4.1. Adsorbent Characterization

4.1.1. FTIR

The FTIR spectra of sewage sludge (SS) before and after adsorption of methylene blue (MB) are shown in Figure 2(a) and (b), while the corresponding peak assignments are summarized in Table 3. The spectra indicate the presence of several functional groups on the sludge surface, including C–O, C=O, C–H, and O–H groups, which may participate in the adsorption process. After MB adsorption, noticeable changes in peak intensity and slight shifts in peak positions were observed, particularly for the C–O, C–H, and O–H stretching bands, indicating possible interactions between dye molecules and functional groups on the adsorbent surface. The shift of the O–H stretching band and changes in the C=O region suggest that hydrogen bonding and other surface interactions may contribute to the adsorption mechanism. These results indicate that oxygen-containing functional groups on the sewage sludge surface play an important role in MB dye adsorption.

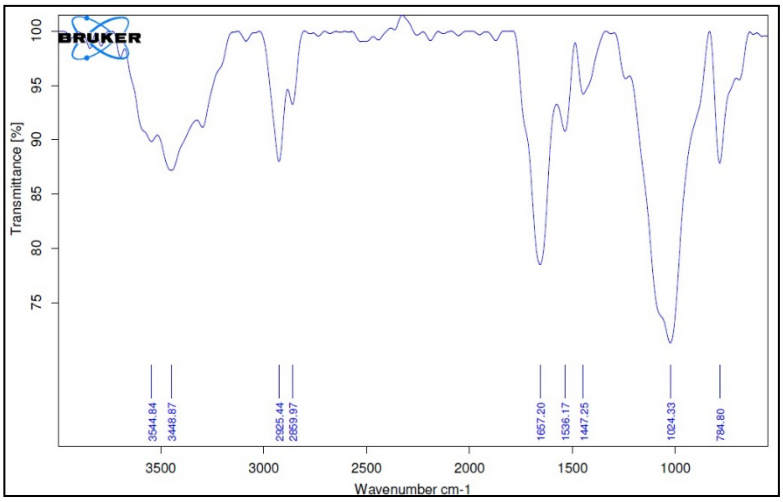

(a)

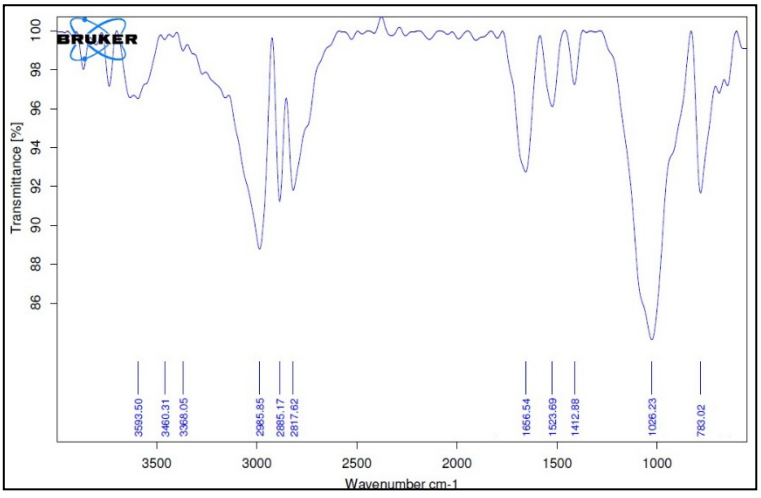

(b)

Figure 2. FTIR analysis (a) before and (b) after adsorption of methylene blue dye

Table 3. FTIR spectral analysis before and after the adsorption of the MB dye

Wavenumber (cm^{-1}) before adsorption	Wavenumber (cm^{-1}) after adsorption	Functional group	Band description	Reference
784.8	783.02	CH_2 scissoring deformation	Aliphatic moieties	[16]
1024.33	1026.23	C-O stretching	Alcohol	[5,17]
1447.25	1412.88	CH_2 rocking	Methylene group	[16]
1536.17 1657.20	1523.69 1656.34	C=O stretching vibrations	Amide group	[17,18]
2859.97 2925.44	2817.62 2885.17 2985.85	C-H stretching	Aliphatic chain	[17]
3448.87 3544.84	3368.05 3460.31 3593.50	-OH stretching vibration	Alcohol	[19]

4.1.2. Field Emission Scanning Electron Microscopy (FESEM)

The surface morphology of the sewage sludge (SS) adsorbent before and after MB adsorption was examined using FESEM at a magnification of 500 nm, as shown in Figure 2. Before adsorption (Figure 3a), the SS surface exhibited a porous and irregular structure with pores of varying shapes and sizes, providing numerous active sites for dye adsorption.

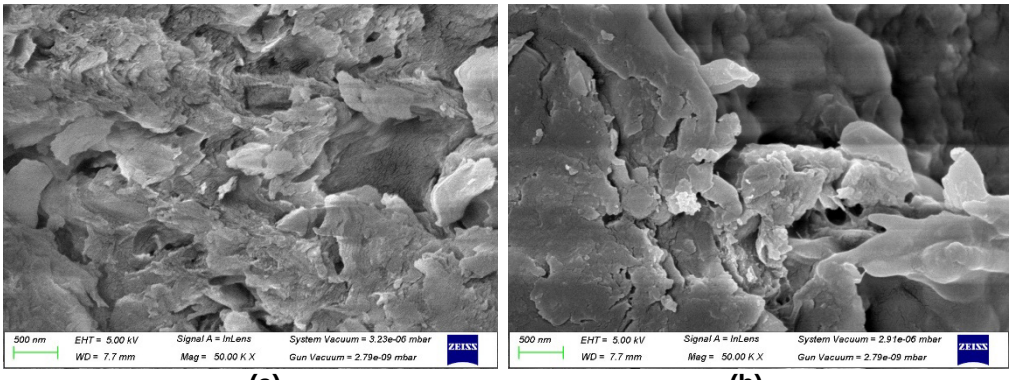

(a) **(b)**

Figure 3. FESEM results for SS (a) before adsorption, (b) after adsorption

After adsorption of MB molecules (Figure 3b), the surface appeared comparatively smoother, and several pores were partially covered or filled, indicating the deposition of dye molecules on the adsorbent surface. These morphological changes suggest that MB adsorption occurred through surface interaction and pore filling within the sludge matrix.

4.1.3. Brunauer–Emmett–Teller (BET)

The textural properties of the sewage sludge adsorbent were characterized using nitrogen adsorption–desorption analysis at 77 K. The adsorption isotherm exhibited a Type II profile, indicating multilayer adsorption behaviour typically associated with materials possessing macroporous structures or limited porosity (Figure 4a and 4b). The BET surface area of the sewage sludge was 1.669 m^2/g, with a total pore volume of 0.00437 cm^3/g and an average pore diameter of 10.47 nm (Table 4). The relatively low surface area is characteristic of untreated sludge materials and may be attributed to the presence of organic matter and mineral components that partially block internal pores.

After adsorption, the BET surface area decreased to 1.131 m^2/g, while the total pore volume decreased to 0.00353 cm^3/g, as shown in Table 4. In contrast, the average pore diameter increased slightly to 12.47 nm. The reduction in surface area and pore volume suggests that adsorbate molecules occupied and partially blocked the available pores of the sewage sludge adsorbent during the adsorption process, indicating effective interaction between the adsorbate molecules and the adsorbent surface.

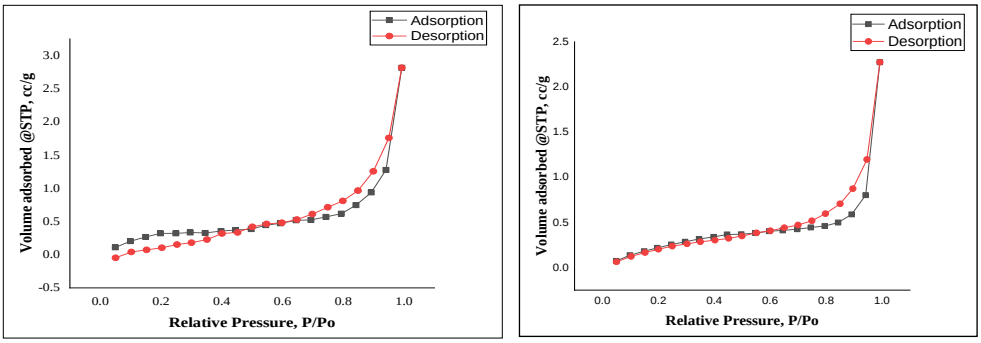

(a) **(b)**

Figure 4. Nitrogen adsorption/desorption isotherm plot of Sewage Sludge before (a) and after adsorption (b)

Table 4. Textural properties of the Sewage Sludge adsorbent before and after adsorption

Sample (Sewage Sludge)	BET Surface Area (m^2/g)	Total pore volume (cm^3/g)	Average Pore diameter (nm)
Before adsorption	1.669	0.00437	10.47
After adsorption	1.131	0.00353	12.47

4.2. Batch adsorption studies

Batch adsorption experiments were carried out to investigate the influence of key operational parameters on the removal of methylene blue using sewage sludge as an adsorbent. The effects of solution pH, adsorbent particle size and dosage, initial dye concentration, and contact time were examined to determine the optimal conditions for adsorption.

4.2.1. Effect of pH

The adsorption capacity and dye solubility are significantly influenced by the pH of the dye solution. This study assessed the MB dye adsorption capacity on sewage sludge across a pH range of 3-11. As depicted in Figure 5(a), the amount of dye removed decreased with rising pH from 3 to 5. From pH 3 to pH 5, the amount of dye eliminated is reduced. The dye removal decreases further when the pH rises from 5 to 7. However, an impressive increase in the sorption capacity with increasing pH was noted, between pH 9 and pH 11. While the highest adsorption was observed at pH 11, the increase in adsorption capacity compared to pH 9 was marginal. Considering the minimal performance disparity and the operational and environmental benefits of functioning at a reduced pH, pH 9 was considered appropriate. Maintaining a pH of 9 aligns with standard wastewater treatment pH ranges, hence reducing the necessity for post-treatment neutralization. To verify the adsorption process spectroscopically, UV–Vis spectra of methylene blue solution at different contact times (for an initial concentration of 10 mg/L) were recorded. As shown in Figure 5(b), the absorbance at 664 nm decreases progressively with increasing contact time, confirming dye uptake by the adsorbent.

The pH-dependent behaviour of MB adsorption can be explained in terms of the point of zero charge (pH_{pzc}). The point of zero charge (pH_{pzc}) of the sewage sludge (adsorbent) was determined using the pH drift method, as shown in Figure 5(c) and found to be 7.6. At pH values higher than 7.6, the sludge surface becomes negatively charged, which enhances attraction toward the positively charged MB dye molecules. Conversely, at pH values lower than pH_pzc, the surface becomes positively charged, resulting in reduced adsorption due to electrostatic repulsion. This explains the observed increase in dye removal efficiency under alkaline conditions, which is similar to several other studies reported for the adsorption of methylene blue [5].

In the present study, a significant shift in solution pH was also observed after the adsorption of methylene blue onto sewage sludge. Regardless of the initial pH, whether acidic (pH 3–5) or alkaline (pH 9–11), the final pH consistently stabilized in the near-neutral range of 6.6 to 7.1. For instance, an initial pH of 3.0 increased to 6.6, while a starting pH of 9.0 decreased to 7.1 after the adsorption process. This convergence toward neutrality reflects a pH-stabilising or

neutralizing effect. Such behaviour is likely due to the acid–base interactions and ion-exchange properties of surface functional groups present in sewage sludge, particularly hydroxyl, carboxylic, and amine moieties, which can either release or absorb protons depending on the solution environment. A similar phenomenon was reported by another study, where sludge-derived biochar exhibited a stabilising effect on pH following the adsorption of both phosphate and methylene blue [18]. This is attributed to residual mineral components and functional groups retained or modified during sludge treatment, which facilitate proton exchange and mitigate extreme pH variations. This pH-regulating property of sewage sludge enhances its practical applicability in real-world wastewater treatment scenarios, ensuring that treated effluents maintain acceptable pH levels for safe discharge or further processing.

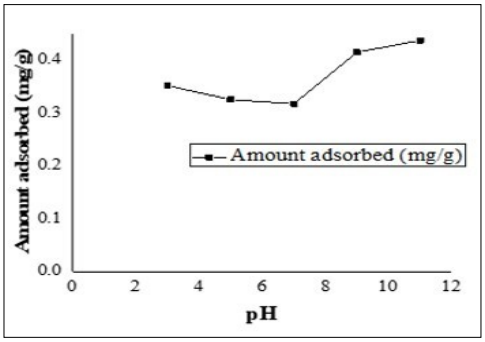

Figure 5(a) Effect of dye solution's pH (0.5 g of SS, $[MB]_i$ = 10 mg /L, V = 50 mL, particle size = 0.5 mm, T = 25°C and shaking speed = 180 rpm)

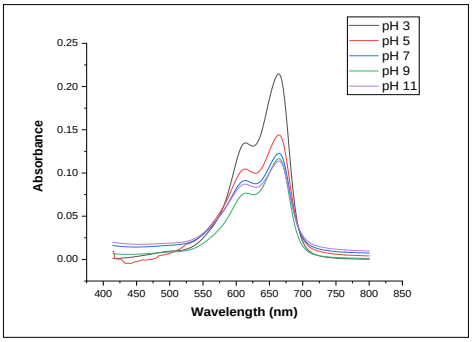

Figure 5(b) UV–Vis spectra of methylene blue solutions after adsorption at different pH using sewage sludge adsorbent.

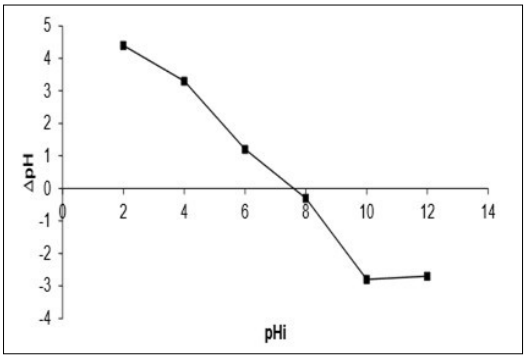

Figure 5(c) Determination of point of zero charge (pH_pzc) of sewage sludge by pH drift method.

4.2.2. Effect of Initial Dye Concentration and Contact Time

The dye solutions were prepared at varying concentrations ranging from 10 to 100 mg/L. The impact of initial dye concentration along with the contact time on dye removal is depicted in Figure 6(a). The results concerning the effect of contact time indicate that the absorbance of MB dye increased significantly as the contact time was extended from 5 minutes to 30 minutes. After 45 minutes, the system reached equilibrium for every concentration. Also, an increase in adsorption capacity was seen with increasing dye concentration, which may be due to increased mass transfer. To verify the adsorption process spectroscopically, UV–Vis spectra of methylene blue solution at different contact times (for an initial concentration of 10 mg/L) were recorded. As shown in Figure 6(b), the absorbance at 664 nm decreases progressively with increasing contact time, confirming dye uptake by the adsorbent.

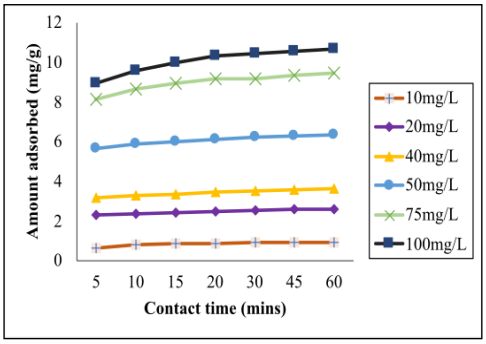

Figure 6(a). Effect of dye concentration and contact time (0.5 g of SS, particle size = 0.5 mm, V = 50 mL, pH =9, T = 25°C and shaking speed = 180 rpm)

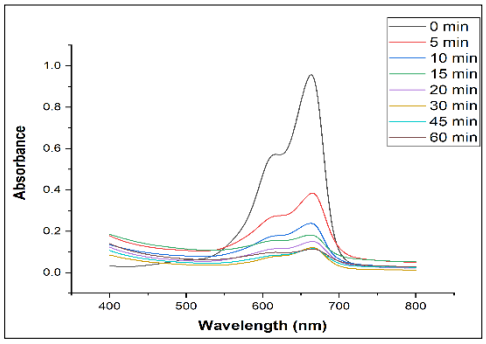

Figure 6(b). Time-dependent UV–Vis spectra of methylene blue solution (10 mg/L) during adsorption onto sewage sludge.

4.2.3. Effect of Particle Size

The sorption capacity of MB was studied at three particle sizes, i.e., 0.25, 0.5, and 1 mm, for which the amount of adsorbed dye was observed. As shown in Figure 7(a), the dye removal capacity increased with lower particle size (0.25 mm) due to increased surface area. However, the difference was not significant, but the MB dye removal capacity increased with increasing contact time and decreasing particle size of the adsorbent. The UV–Vis spectra of the residual dye solutions obtained for different adsorbent particle sizes are shown in Figure 7(b), where the decrease in absorbance at 664 nm indicates enhanced adsorption with decreasing particle size.

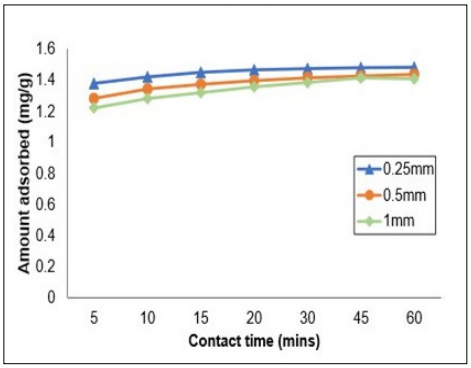

Figure 7(a). Effect of adsorbent particle size and rate of adsorption (0.5 g of SS, $[MB]_i$ = 10 mg /L, V = 50 mL, pH = 9, T = 25°C and shaking speed = 180 rpm)

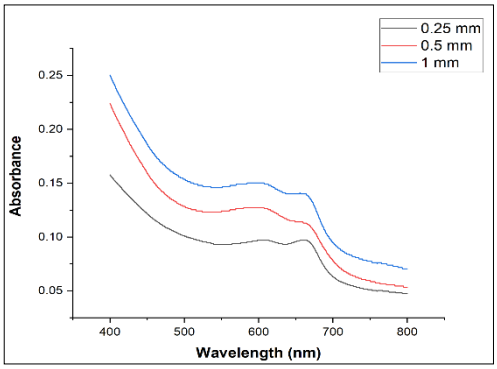

Figure 7(b). UV–Vis spectra of methylene blue solutions after adsorption using different particle sizes of sewage sludge (contact time 30 min)

4.2.4. Effect of Adsorbent Amount

The effect of the adsorbent amount for MB dye was studied by varying the adsorbent amount, ranging from 0.25 g to 1 g of SS in 50 mL of dye solution (10 mg/L).

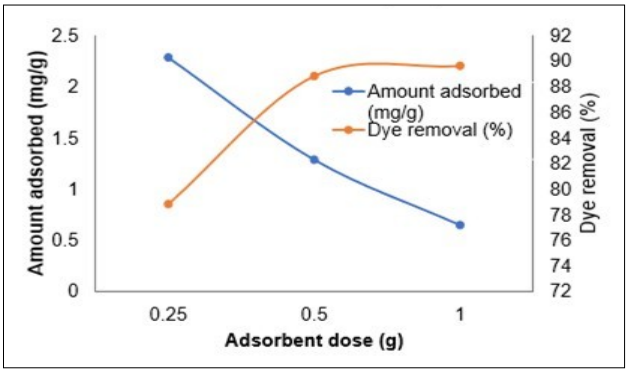

Figure 8. Effect of adsorbent dosage on the adsorption of methylene blue onto sewage sludge. ($[MB]_i$ = 10 mg/L, particle size = 0.5 mm, V = 50 mL, pH =9, T = 25°C and shaking speed = 180 rpm)

As the overall concentration of dye in the solution remains constant, the addition of adsorbent mass reduces the ratio of dye to adsorbent, which suggests a lower dye adsorption per gram of adsorbent, as shown in Figure 8. As a result, while the overall dye removal percentage increases due to the increased number of available active sites, specific adsorption capacity reduces.

4.3. Adsorption Isotherm Models

Adsorption isotherms were studied in batch experiments by varying the dye concentrations at 10 and 20. 30, 50, 75, 100, 150, and 200 mg/L. Contact time, adsorbent dose, pH, and temperature were fixed at 45 min, 0.5 g, 9, and 25 ±5 °C, respectively, in the experimental study.

The equilibrium adsorption data were analyzed using Langmuir, Freundlich, Temkin, and Harkin-Jura isotherm models. The corresponding linear plots are presented in Figure 9 (a-d). The fitting parameters of the isotherm models were determined from these linear plots, and the results are summarized in Table 5.

The Langmuir adsorption parameters were determined using equations mentioned in Table 1. MB dye showed a maximum adsorption efficiency of 14.08 mg/g. The favorability of adsorption was further evaluated using the dimensionless separation factor (R_L). The R_L values calculated using the Langmuir constant (K_L = 0.26 L mg^{-1}) were found to be 0.039 for the studied concentration range (10 to 200 mg/L), indicating favourable adsorption of methylene blue onto sewage sludge. The value of the separation factor (R_L) ranges from 0.03 to 0.3. The decrease in R_L with increasing initial concentration indicates favourable adsorption at higher concentrations. The higher K_L value compared with other studies indicates a stronger adsorption affinity [11]. Additionally, a lower R_L value of 0.039 for this study compared to the value reported by Kaya (2025) confirms the adsorption to be more favourable [11]. The R^2 value of 0.991 indicates the Langmuir isotherm to be the best fit for explaining the adsorption process.

The parameters for the Freundlich isotherm were also evaluated using the equations mentioned in Table 1. The value of the Freundlich constant (K_F) was 2.53 L/mg, the heterogeneity factor (n) was found to be in the range 1-10 (1.314), and a lower value of $1/n$ (0.76) indicates that the adsorption is favourable and moderate and the surface is heterogeneous compared to the value reported by Hayfron et al. (2025), n = 0.89 for zeolite prepared from mixing kaolinite clay and rice husk ash [4]. The current results indicate higher adsorption intensity (n>1). The R^2 value of MB dye for the Freundlich isotherm was 0.965, which is lower than that of the Langmuir isotherm (0.991), suggesting that this model does not fit the equilibrium data well.

For the Temkin isotherm model, the values of the parameters mentioned in Table 1 were calculated. The equilibrium binding constant (A_T) value was 2.31 L/mg, and the heat of adsorption constant (b_T) was 0.843 KJ/mol. A higher A_T value implies that there was a strong interaction between the dye and the adsorbent. According to Nandiyanto et al. (2023), if the value of b_T is below 8 kJ, the adsorption process would be governed by physisorption, while if the value is above 8 kJ, then by chemisorption [12]. Therefore, according to this study, the adsorption of MB onto SS was controlled by physisorption due to the lower b_T value of 3.04. Having higher b_T and A_T values suggests that the adsorption process might have occurred through a combination of physical and chemical sorption. The correlation coefficient value of MB dye for the Temkin isotherm is 0.981.

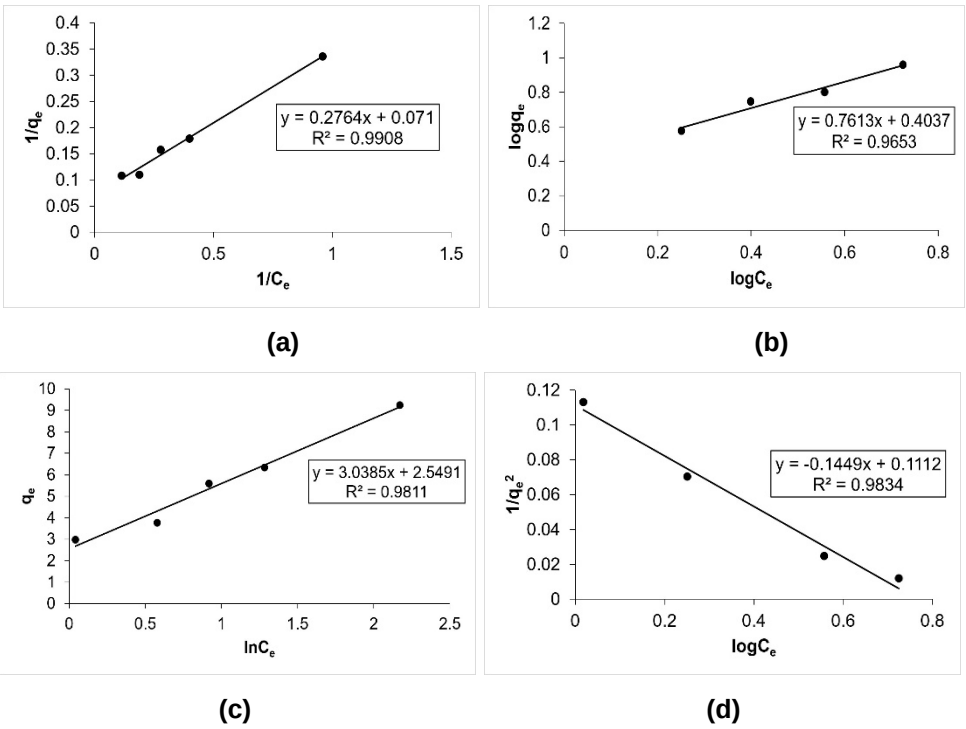

Figure 9. Experimental adsorption isotherm showing the relationship between equilibrium adsorption capacity (q_e) and equilibrium dye concentration (C_e) for methylene blue adsorption onto sewage sludge using (a) Langmuir, (b) Freundlich, (c) Temkin, and (d) Harkin-Jura

The Harkin-Jura isotherm parameters were calculated using equations given in Table 1. The values of Harkin-Jura constants *A* (6.901 mg/g) suggested a moderate adsorption capacity of the adsorbent, and constant *B* (0.767) suggested the presence of multilayer adsorption and that the adsorbent does not possess uniform energy distribution. The value of the correlation coefficient (0.983) for the model indicated an effective multilayer adsorption due to a heterogeneous surface.

Table 5. Isotherm parameters for MB dye adsorption on sewage sludge

Isotherm Models	Langmuir	Freundlich	Temkin	Harkin-Jura
Parameters and their values	q_{max}-14.08 mg/g	*n*- 1.314	A_T-2.31 L/mg	*A*- 6.901 mg/g
	K_L- 0.26 L/mg	*1/n*- 0.761	B_T-3.04	*B*- 0.767
	R_L- 0.039	K_F- 2.53 L/mg	b_T- 0.843 kJ/mol	R^2- 0.983
	R^2 - 0.991	R^2 - 0.965	R^2 - 0.981	

The maximum adsorption capacity (q_{max}) of different non-conventional low-cost adsorbents utilised for dye adsorption was compared, and the comparative data with sewage sludge are summarised in Table 6. The adsorption capacity achieved by the adsorbent was determined by the Langmuir isotherm, yielding a value of 14.08 mg/g. This performance stands out, giving strong competition to other listed adsorbents (Table 6). A comparison of the adsorption capacity of SS used in the present study for MB removal from aqueous solution with other low-cost adsorbents reported by various researchers is shown in Table 6. It can be concluded that even in its natural state, without any modification, SS was found to be a better alternative for the efficient removal of MB dye from aqueous solutions as compared to other adsorbents reported for the removal of MB.

Table 6. Comparison between the adsorption capacities of different adsorbents for dye removal

Adsorbent	Dye	Maximum adsorption capacity (mg/g)	Reference
Coconut dreg	Methylene Blue	5.72	[20]
	Brilliant Red Remazol	3.76	
Lemon peel	Eosin	8.24	[21]
Coconut husk	Crystal Violet	0.73	[22]
Nanobentonite	Malachite Green	13.8	[23]
Graphite and nano-bentonite clay	Basic Blue 5	2.33	[24]
Sewage sludge	Methylene Blue	**14.08**	**This work**

4.4. Adsorption Kinetics

Adsorption kinetics experiments were performed by adding 0.5 g of sewage sludge (SS) to 50 mL of methylene blue (MB) aqueous solution with an initial concentration of 25 mg/L at temperatures ranging from 25–45 ± 5°C. Samples were withdrawn at predetermined contact times (5, 10, 15, 20, 30, 45, 60, 90, and 120 min), and the absorbance was measured to determine the residual dye concentration.

The predicted theoretical kinetics and the data for the experimental equilibrium of MB on SS are shown in Figure 10. An attempt was made to plot ln (q_e-q_t) against time (t) as seen in Figure 10(a), resulting in undefined negative values, rendering the first-order kinetic model unfeasible and suggesting that the first-order linearised equation is unsuitable to describe the sorption process (Table 7).

According to the experimental data shown in Table 7 and Figure 10(b), the pseudo-second-order model was found to be the best fit to the adsorption equilibrium data with a correlation coefficient value of 0.999, which is greater than that of the pseudo-first-order (0.982), Intra-particle diffusion (0.8087) and Elovich models (0.931), which signifies possibility of chemisorption involved in sorption process. The pseudo-second-order model provided the best description of the adsorption kinetics with a higher correlation coefficient (R^2 = 0.999). In addition, the calculated adsorption capacity (3.08 mg/g) obtained from the pseudo-second-order model was in good agreement with the experimentally determined q_e value (3.14 mg/g), further confirming that this model adequately describes the adsorption process. The pseudo-second order model predicted an adsorption capacity of 3.08 mg/g, which was closest to the experimental value of 3.14 mg/g.

A greater value of the intra-particle diffusion rate constant (k_{id}) suggested that the adsorbent quickly diffuses into the pores, and as the intercept denoting the boundary layer effect (C_i) is not equal to 0, it can be concluded that intra-particle diffusion is not the sole rate-limiting mechanism (Table 7, Figure 10(c)).

Table 7. Kinetic parameters for MB dye adsorption under optimised conditions

Kinetic Models	PFO	PSO	Elovich	IPD
Parameters and their values	q_e (mg/g) = -0.456	q_e (mg/g) = 3.14	α (mg/g.min) = 141800	K_{id} (mg/g.min$^{1/2}$) = 2.5711
	k_1 (min^{-1}) = -0.051	k_2 (g/mg.min) = 0.2011	β (g/mg) = 5.83	C_i = 0.0569
	R^2 = 0.982	R^2 = 0.999	R^2 = 0.931	R^2 = 0.8087

The results of the Elovich model indicated a higher *α* value (141,800 mg/g.min), as shown in Table 7 and Figure 10(d), which suggests that the adsorption was rapid, indicative of adsorption following chemisorption.

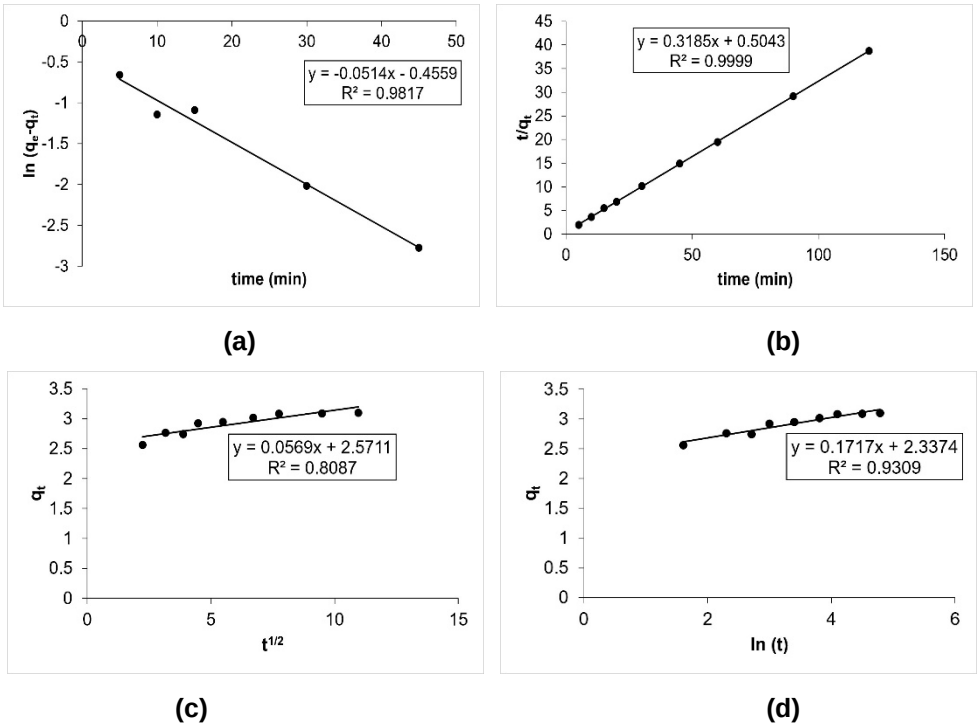

Figure 10. Kinetic study for MB dye adsorption using (a) PFO, (b) PSO, (c) IPD, and (d) Elovich models

4.5. Thermodynamics study

To evaluate the thermodynamic feasibility and nature of methylene blue adsorption onto sewage sludge, adsorption experiments were conducted at different temperatures (298–318 K). The thermodynamic parameters were calculated from the equilibrium distribution coefficient (K_d) using the Van't Hoff relationship, and the results are presented in Table 8. The values of K_d decreased with increasing temperature, indicating a reduction in adsorption capacity at higher temperatures and suggesting that the adsorption process is

exothermic in nature. This trend is also reflected in the decrease in adsorption capacity (q_e) from 3.080 to 2.227 mg/g as the temperature increased from 298 to 318 K.

The negative values of Gibbs free energy change ($\Delta G°$) obtained at all studied temperatures indicate that the adsorption of methylene blue onto sewage sludge is a spontaneous process. Furthermore, the negative value of the enthalpy change ($\Delta H°$) confirms the exothermic nature of the adsorption process, indicating that lower temperatures favour dye uptake. The magnitude of the enthalpy change ($\Delta H° = -46.48$ kJ/mol) suggests relatively strong interactions between methylene blue molecules and the functional groups present on the sewage sludge surface, indicating that the adsorption process may involve strong physical interactions and possible surface complexation. The entropy change ($\Delta S°$) was found to be negative, suggesting a decrease in randomness at the solid–solution interface during adsorption. This decrease in randomness may be attributed to the orderly arrangement of dye molecules on the surface of the adsorbent during the adsorption process. Similar thermodynamic behaviour for methylene blue adsorption has been reported in previous studies using various low-cost adsorbents [25, 26]. Overall, the thermodynamic parameters indicate that the adsorption of methylene blue onto sewage sludge is spontaneous and exothermic, with adsorption being more favourable at lower temperatures.

Table 8. Thermodynamic parameters for methylene blue adsorption onto sewage sludge at different temperatures

Temperature (K)	C_e (mg/L)	q_e (mg/g)	K_d	$\Delta G°$ (kJ/mol)	$\Delta H°$ (kJ/mol)	$\Delta S°$ (J/mol.K)
298	0.707	3.080	4.36	-3.49	-46.48	-144.23
308	1.154	2.277	1.97	-2.05	-	-
318	1.657	2.227	1.34	-0.60	-	-

The thermodynamic parameters were further analyzed using the Van't Hoff plot by plotting ln K_d against 1/T, as shown in Figure 11. The slope and intercept of the linear plot were used to determine the enthalpy change ($\Delta H°$) and entropy change ($\Delta S°$), respectively. The linear relationship obtained confirms the applicability of the thermodynamic model for describing the adsorption behaviour of methylene blue onto sewage sludge.

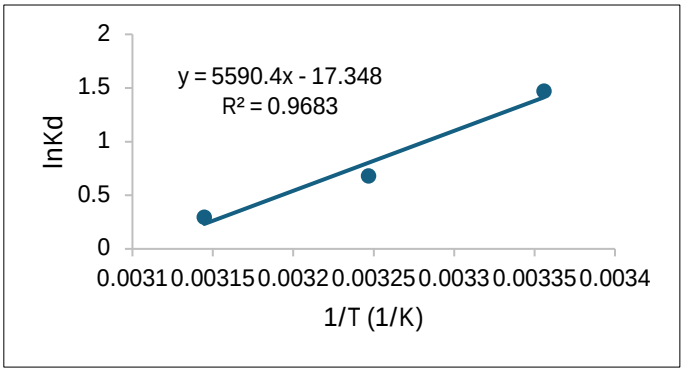

Figure 11. Van't Hoff plot (ln K_d versus 1/T) for methylene blue adsorption onto sewage sludge.

5. CONCLUSIONS

The present study investigated the potential use of secondary treated sewage sludge as a low-cost adsorbent for the removal of methylene blue from aqueous solutions. Characterization of the material using FTIR, SEM, and BET analyses revealed the presence of surface functional groups, porous morphology, and adequate surface area that provide suitable adsorption sites for dye molecules. The adsorbent exhibited a point of zero charge (pH_{pzc}) of 7.6, which explains the enhanced adsorption of the cationic dye under alkaline conditions due to the development of negatively charged surface sites.

Batch adsorption experiments demonstrated that operational parameters such as pH, adsorbent dosage, contact time, particle size, and initial dye concentration significantly influence the adsorption process. Optimal conditions were observed at pH 9, with 0.5 g of sewage sludge in 50 mL of 10 mg/L dye solution and a contact time of 30 minutes. Although the highest dye removal efficiency was observed at pH 11, pH 9 was considered the optimum pH due to the minimal difference in removal performance and its practical advantage of producing a near-neutral final pH, thereby reducing post-treatment adjustment requirements. The adsorption equilibrium data showed good agreement with the Langmuir isotherm model, with a maximum adsorption capacity of 14.08 mg/g, while the adsorption kinetics followed the pseudo-second-order model, indicating that the adsorption process is governed by interactions between dye molecules and active sites on the sludge surface.

Thermodynamic analysis based on temperature-dependent equilibrium data and the Van't Hoff plot indicated that the adsorption process is spontaneous and exothermic. The negative values of ΔG° confirmed the feasibility of the process, while the negative values of ΔH° and ΔS° suggested an exothermic adsorption process accompanied by decreased randomness at the solid–solution interface.

An additional observation was the pH-stabilizing behaviour of the adsorbent, where the final solution pH tended to converge toward near-neutral values regardless of the initial pH. This buffering-like effect is likely associated with the presence of surface functional groups and mineral constituents in the sludge and further enhances its practical applicability for wastewater treatment.

Overall, the results demonstrate that untreated sewage sludge can serve as an effective and environmentally sustainable adsorbent for methylene blue removal from contaminated water. The utilization of sewage sludge not only contributes to wastewater treatment but also promotes waste valorization and resource recovery. Future studies may focus on environmentally benign modification strategies to further enhance the adsorption performance of the material.

ACKNOWLEDGEMENTS

The infrastructural financial support under the CURIE programme from the WISE-KIRAN division of the Department of Science and Technology, New Delhi, India, to IIS (deemed to be University), Jaipur, India (File No. DST/CURIE-02/2023/IISU) is gratefully acknowledged.

REFERENCES

1. V. K. Parida; N. Singh; M. Priyadarshini; P. Kumari; D. Datta; A. Tambi; *J. Ind. Eng. Chem.,* **2025**, *150*, 247–264.
2. R. Al-Tohamy; S. S. Ali; F. Li; K. M. Okasha; Y. A. Mahmoud; T. Elsamahy; H. Jiao; Y. Fu; J. Sun; *Ecotoxicol. Environ. Saf.,* **2022**, *231*, 113160.
3. I. Susanti; H. B. N. Sajidah; S. R. Rosdiana*;* IOP Conf. Ser.: Earth Environ. Sci., **2024**, *1425*, 012009.
4. J. Hayfron; S. Jääskeläinen; S. Tetteh; *Heliyon,* **2024**, *11*, 41325.
5. M. A. Ibrahim; A. Salama; F. Zahran; M. S. Abdelfattah; A. Alsalme; M. Bechelany; A. Barhoum; *Front. Chem.*, **2024***; 12*, 1330810.
6. S. Moosavi; C. W. Lai; S. Gan; G. Zamiri; P. O. Akbarzadeh; M. R. Johan; *ACS Omega*, **2020**, *5*, 20684–20697.

7. M. Dhamsaniya; D. Christian; M.A. Shabiimam; Issues of Sustainable Sludge Handling and Management in the Wastewater Sector: A Review. In *Innovation in Smart and Sustainable Infrastructure*, Volume 2. ISSI **2022**. Lecture Notes in Civil Engineering, vol 485; D. Patel; B. Kim; D. Han Eds.; Springer, Singapore, 2024, pp. 55–68.
8. V. Singh; H. C. Phuleria; M. K. Chandel; *J. Clean. Prod.*, **2020**, *276*, 122538.
9. A. Raj; A. Yadav; A. P. Rawat; A. K. Singh; S. Kumar; A. K. Pandey; R. Sirohi; A. Pandey; *Environ. Technol. Innov.,* **2021**, *23*, 101556.
10. M. Keshawy; R. S. Kamal; A. E. Abdelhamid; A. Labena; A. Amin; A. M. Hasan; M. E. Abdel-Raouf; *Int. J. Environ. Sci. Technol.,* **2025**, *22*, 8895-8918.
11. H. Kaya; *Cellulose. Chem. Technol.*, **2025**, *59*, 441-450.
12. A. B. D. Nandiyanto; M. Fiandini; D. A. Fadiah; P. A. Muktakin; R. Ragadhita; W. C. Nugraha; T. Kurniawan; M. R. Bilad; J. Yunas; A. S. M. Al Obaidi; *J. Adv. Res. Fluid Mech. Therm. Sci.,* **2023**, *105*, 41-58.
13. F. Mohamed; M. Shaban; S. K. Zaki; M. S. Abd-Elsamie; R. Sayed; M. Zayed; N. Khalid; S. Saad; S. Omar; A. M. Ahmed; A. Gerges; H. R. Abd El-Mageed; N. K. Soliman; *Scientific Reports*, **2022,** *12*, 18031.
14. O. A. Abdel Moamen; A. A. Mohammed; H. A. Ibrahim, A. M. El-Kamash; *Geoenviron. Disasters.,* **2025***, 12*, 29.
15. N. Jawad; T. M. Naife; *Iraqi J. Chem. Pet. Eng.*, **2022**, *23*, 59-69.
16. J. de Oliveira Silva; G. Rodrigues Filho; C. da Silva Meireles; S. D. Ribeiro; J. G. Vieira; C. V. da Silva; D. A. Cerqueira; *Thermochim. Acta*, **2012,** *528*, 72-75.
17. H. Messaoudi; A. Koukouch; I. Bakhattar; M. Asbik; S. Bonnamy; E. G. Bennouna; T. Boushaki; B. Sarh; A. Rouboa; *Energies*, **2024**, *17*, 582.
18. L. Romero; T. Joglar; P. Oulego; S. Collado; M. Díaz; *J. Environ. Man.*, **2025**, *391*, 126380.
19. Y. N. Teixeira; J. M. Menezes; R. N. Teixeira; F. J. Paula Filho; T. M. Oliveira; *Textiles*, **2023**, *3*, 52-65.
20. H. Shukor; A. Z. Yaser; N. F. Shoparwe; M. MohdZainiMakhtar; N. Mokhtar; *Int. J. Chem. Eng.*, **2022**, *2022*, 1–11.
21. A. Bukhari; I. Ijaz; H. Zain; E. Gilani; A. Nazir; A. Bukhari; S. Raza; S. Hussain; S. S. Alarfaji; Y. Naseer; *Arab. J. Chem*., **2022**, 15, 103873.
22. M. S. Imran; T. Javed; I. Areej; M. N. Haider; *Water Sci. Technol.*, **2022**, *85*, 2295-2317.
23. M. T. Moustafa; *Scientific Reports,* **2023**, *13*, 4493.
24. N. Elshemy; H. Mashaly; S. Elhadad; *Pigment Resin Technol.,* **2023**, *53*, 900–910.
25. L. Ykhlef; H. Ghania; H. Salah; *Cellul. Chem. Technol.*, **2024**, *58*, 1135.
26. M. F. M. Yusop; A. Aziz; M. A. Ahmad; *Arab. J. Chem.*, **2022**, *15,* 104081.